$^{90}Zr(p,p')^{90}Zr^*$ Reaction at 40 MeV

R. A. Hinrichs† and D. Larson‡
Cyclotron Laboratory, § Michigan State University, East Lansing, Michigan 48823

B. M. Preedom¶
Department of Physics, University of South Carolina, Columbia, South Carolina 29208

W. G. Love‖
Department of Physics, University of Georgia, Athens, Georgia 30601

F. Petrovich
*Lawrence Berkeley Laboratory,** University of California, Berkeley, California 94720*
(Received 20 November 1972)

Differential cross sections for the excitation of the 0^+ (1.75-MeV), 2^+ (2.18-MeV), 5^- (2.32-MeV), 4^+ (3.08-MeV), 6^+ (3.45-MeV), 8^+ (3.60-MeV), and the 2^+ (3.31-MeV) levels in ^{90}Zr by 40-MeV protons have been measured between 15° and 115°. The data are compared with the results of distorted-wave (DWA) collective-model calculations and DWA microscopic-model calculations. Both macroscopic and microscopic treatments of core polarization are considered. Effects from noncentral components in the projectile-target interaction have been investigated and an imaginary central component has been included in this interaction in the cases where a completely microscopic model is used for the target nucleus. A coupled-channels calculation has been performed in order to investigate multiple excitation contributions to the cross section for the 0^+ (1.75-Mev) state.

I. INTRODUCTION

In recent years the $^{90}Zr(p,p')^{90}Zr^*$ reaction has been a favorite subject for physicists working on the microscopic model for inelastic proton scattering.[1-3] The main reason for this is the substantial range of multipolarities available in the transitions from the ground state of this nucleus to its first excited 0^+, 2^+, 4^+, 5^-, 6^+, and 8^+ states, whose wave functions consist mainly of two protons distributed in the $2p_{1/2}$- and $1g_{9/2}$-shell model orbitals. The present paper reports on a new experimental study of this nucleus carried out with 40-MeV incident protons. Differential cross sections have been measured for the excitation of the six states named above, as well as for the excitation of the state at 3.31 MeV. These data, combined with the results of earlier experiments at 12.7,[2] 18.8,[1] and 61.2 MeV,[3] give a reasonably complete picture of the energy dependence of the cross sections from 10–60 MeV. The angular distribution for the $L=0$ transition, however, had previously been measured only at the comparatively low energy of 12.7 MeV.[2] Thus the present measurement significantly extends our knowledge of this monopole transition and can provide an additional test for various aspects of the reaction theory.

The microscopic model for inelastic proton scattering has undergone considerable development in recent years. It is now fairly well established that cross sections can be understood in calculations with "realistic interactions,"[4-9] provided that "knock-on" exchange contributions are included and reasonable target wave functions are used. Most calculations have previously considered only the real central components of the projectile-target interaction. However, recent studies have pointed out that the shapes of differential cross sections can be improved by including an imaginary component in the interaction[10,11] and also that the two-body spin-orbit force may be important for transitions of high multipolarity.[12]

In the case of ^{90}Zr, reasonable target wave functions require consideration of core polarization effects.[2,3] This can be done using macroscopic[13,14] or microscopic[7,15,16] models for the core. In the first model the contributions from core polarization are described in terms of a single parameter which can be treated phenomenologically or determined from other data such as effective charges when they are available. In the second model, core-excited admixtures in the valence wave functions are estimated perturbatively using "realistic" coupling interactions. It is interesting to note that inelastic scattering is one of the few methods by which the effect of core polarization in transitions of high multipolarity can be studied.

The data from the present experiment have been analyzed using both the collective model and the microscopic model. The deformation parameters

obtained from the collective-model analysis have been compared with those from earlier experiments.[1-3] In the microscopic-model analysis, both macroscopic and microscopic treatments of the core have been considered and the effect of the imaginary and spin-orbit components in the projectile-target interaction have been investigated.

II. EXPERIMENT

The data were obtained using a 40-MeV proton beam from the Michigan State University sector-focused cyclotron. The ^{90}Zr target was a rolled, 2.0-mg/cm^2 self-supporting foil of 96% isotopic enrichment. The scattered protons were analyzed with an Enge split-pole spectrograph (using an acceptance aperture of 2°) and recorded on Kodak NTB 25-μm emulsions. Stainless-steel absorbers were used in front of the plates to stop other particles of greater stopping power than protons. Because of the interest in both the weakly excited 0^+ state at 1.75 MeV and the 2^+, 4^+, 6^+, 8^+ multiplet, three exposures of various duration were taken at each scattering angle. The runs were normalized to the integrated charge collected in the Faraday cup. Checks for target nonuniformity effects were made by using a Si(Li) monitor counter placed at 90° to the beam which detected the elastically scattered protons. The resolution obtained was 20 keV full width at half maximum (FWHM).

The emulsions were scanned in those regions where the excited states of interest could be counted on one of the three exposures. The longest exposure was used primarily for counting the 8^+ (3.60-MeV) and 0^+ (1.75-MeV) states; in the latter case the cross section dropped to 0.1 μb/sr. Because of its small cross section, only the use of emulsion plates allowed us to observe the 0^+ state. With a conventional Si(Li) detector in a scattering chamber, the tail of the elastic peak from slit scattering and from reactions within the detector washes out the 0^+ peak. With a Si position-sensitive detector or wire proportional counter used in a spectrograph, the signal for the lightly ionizing protons is too close to the noise level for the state to be observed. Also, good resolution of the spectrograph system was necessary, since low-lying states in other Zr isotopes present in the target (0.5 to 0.9%) appeared as strongly excited as the 0^+ state.

The energy level diagram of ^{90}Zr is shown in Fig. 1, as taken from Ref. 3 and Lederer, Hollander, and Perlman.[17] Differential cross sections were obtained in this experiment in 5° steps for scattering angles from 15 to 115° for the 0^+ (1.75-), 2^+ (2.18-), 4^+ (3.08-), 6^+ (3.45-), 8^+ (3.60-), 5^- (2.32-), and 2^+ (3.31-MeV) states. Even for the short exposures it was impossible to count the tracks in the peak for the 3^- state, so that state is not included in our analysis.

III. ANALYSIS

A. General

The cross sections for all the levels considered in this experiment were calculated in the distorted-wave approximation (DWA). In addition the cross section for the first excited 0^+ state was calculated in a coupled-channels approximation. For both types of calculations, the optical-model parameters were taken from Table II of Fricke *et al.*[18] This set of parameters represents the best fit to

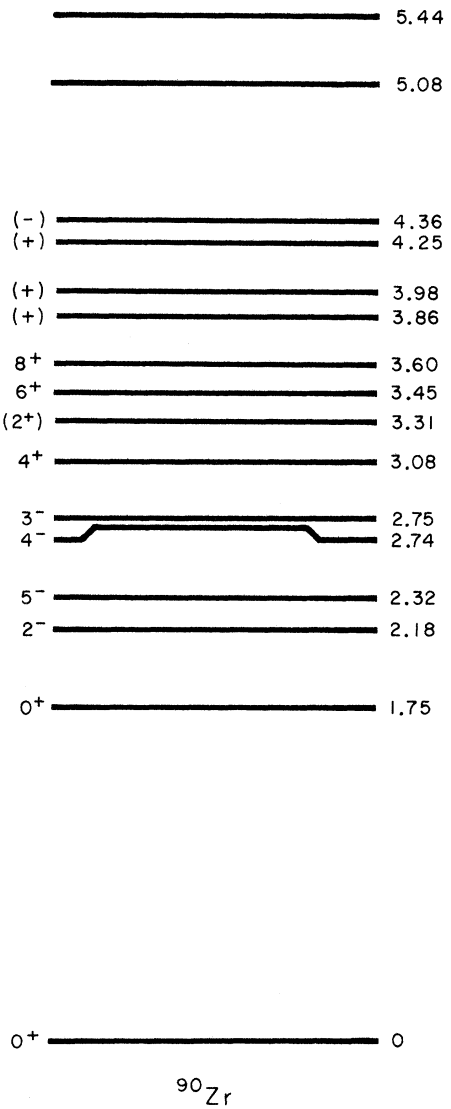

FIG. 1. Energy level diagram of states in ^{90}Zr.

both polarization and cross-section data for the elastic scattering of protons by ^{90}Zr at a bombarding energy of 40 MeV.

Detailed descriptions of the formalisms for both distorted-wave and coupled-channel calculations are given elsewhere.[8, 19, 20] Only those features of the two methods which are particularly relevant to the present analysis will be discussed.

B. Collective-Model Analysis

Although the primary motivation for this experiment was to learn about the microscopic structure of the low-lying levels of ^{90}Zr and the associated reaction mechanism for exciting these states, it is interesting to see how well a simple (one-parameter) vibrational-collective model describes these presumed "shell-model" transitions in the DWA. In this model the low-lying states are taken to be single-phonon states relative to the ^{90}Zr ground state. The resulting form factor is essentially a deformation parameter (β_L) times the radial derivative of the optical potential. Unless stated otherwise, both the real and imaginary (but not the spin-orbit) parts of the optical potential are assuming to undergo vibrations characterized by the same deformation parameter. Coulomb excitation is included for the quadrupole transitions.

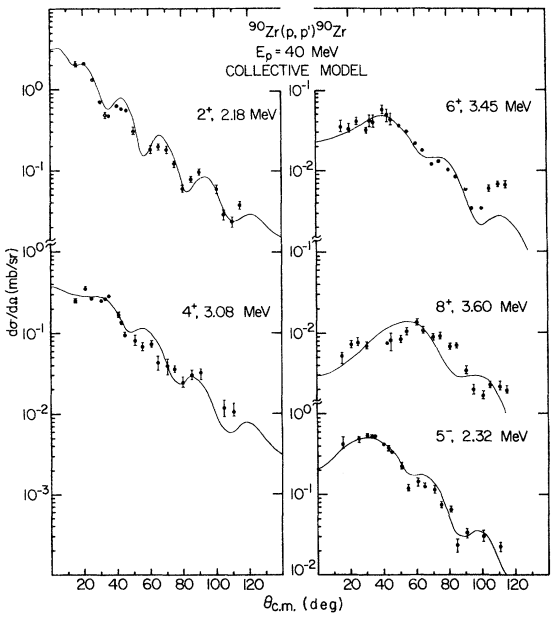

FIG. 2. Collective-model fits to the excitation of the lowest 2^+, 4^+, 6^+, 8^+, and 5^- levels at a proton bombarding energy (E_p) of 40.0 MeV.

1. *Lowest 2^+, 4^+, 6^+, 8^+, and 5^- States*

Figure 2 shows a comparison between the experimental cross sections and the results predicted by the collective model. With the possible exception of the 8^+ state, the shapes of the experimental angular distributions are in reasonable if not good agreement with the predictions of this simple model. The extent to which this model explains the energy dependence of the observed cross sections is indicated in Table I which shows a comparison of the deformation parameters obtained at proton bombarding energies of 12.7, 18.8, 40.0, and 61.2 MeV. The values at 12.7, 18.8, and 61.2 MeV are from Refs. 2, 1, and 3, respectively. The β_L extracted at 40 and 61.2 MeV are quite consistent. The β_L at the lower energies tend to be larger than those at the higher energies particularly for the large L transfers. This may reflect the fact that the macroscopic collective model incompletely accounts for exchange effects in inelastic scattering which are known[4-9] to be most important for large L transfers and for low bombarding energies. Another possible explanation for these discrepancies might be multiple excitation processes.

While the collective model is thought to be inappropriate for the description of the excitation of these levels, its success in describing the angular distributions cannot be denied. Even for these states, β_L at least serves as a useful parameter describing the excitation of these levels.

2. *State at 3.31 MeV*

As shown in Fig. 3 the excitation of this state is described reasonably well by an angular momentum transfer of $L=2$. As seen in Table I the energy dependence of the required β_L is unusually large for $L=2$. As already pointed out,[3] the spin transfer (S) can be either 0 or 1 for the inelastic scattering of spin-$\frac{1}{2}$ particles, so that J of this level is only restricted to be 1^+, 2^+, or 3^+. How-

TABLE I. Deformation parameters (β_L).

E_x (MeV)	J^π	E_p (MeV) 12.7 [a]	18.8 [b]	40.0	61.2 [c]
2.18	2^+	0.075	0.07	0.071	0.068
2.32	5^-	0.09	0.075	0.057	0.058
3.08	4^+	0.053	0.04	0.039	0.040
3.31	(2^+)	0.06	···	0.032	0.034
3.45	6^+	0.04	0.03	0.021	0.022
3.60	8^+	···	0.035	0.014	0.013

[a] Reference 2.
[b] Reference 1.
[c] Reference 3.

ever, Bingham, Halbert, and Bassel[21] have seen this state in an (α, α') experiment on ^{90}Zr at $E_\alpha = 65$ MeV and find $\beta_2 = 0.035$ which is consistent with the value obtained here. Although α particles can also excite states of unnatural parity,[22] the mechanisms by which they do so are different than those for protons (no $\vec{\sigma}_1 \cdot \vec{\sigma}_2$ force for example). Consequently, a spin assignment of 2^+ for this state seems most likely.

3. *Excited 0^+ State at 1.75 MeV*

Although the vibrational model indicates that a breathing mode is the most appropriate description for the excitation of collective monopole states, the collective-model calculation reported here uses the same form factor as for the $L \neq 0$ transfers. This amounts to ignoring volume conservation.[2] Since there is reason[2] to believe this is not a simple breathing mode anyway, this form factor is used mainly for comparison with the other multipoles. Figure 4 shows a comparison of this calculation with experiment. The fit is poor except for the first peak which is well described. The monopole deformation parameter (β_0) is found to be 0.004. The corresponding β_0 at 12.7-MeV proton bombarding energy[2] is 0.03. This strong energy dependence will be discussed in Sec. III C 1. Also shown in Fig. 4 is a calculation assuming an $L = S = 1$ excitation, using the same form factor, which is clearly out of phase with the first maximum. Although such unnatural-parity excitations require an extension of the usual collective model, they arise in a natural way[22,23] when velocity-dependent forces are present. This result is particularly interesting in light of the recently found importance[24] of two-step processes in the excitation of this state by tritons[25] in which the $L = S = 1$ amplitudes give rise to an angular distribution in *better* agreement with experiment than that predicted by $L = 0$. These processes are not expected to be important in proton scattering since the dominant intermediate states are believed[24] to arise from the projectile picking up one of the valence protons.

C. Shell-Model Analysis

In a shell-model or microscopic description of inelastic scattering, the form factor[4-9] for the direct amplitude is obtained by folding the projectile–bound-nucleon interaction into the relevant shell-model transition density. Exchange amplitudes require the off-diagonal elements, $\rho(\vec{r}, \vec{r}')$,

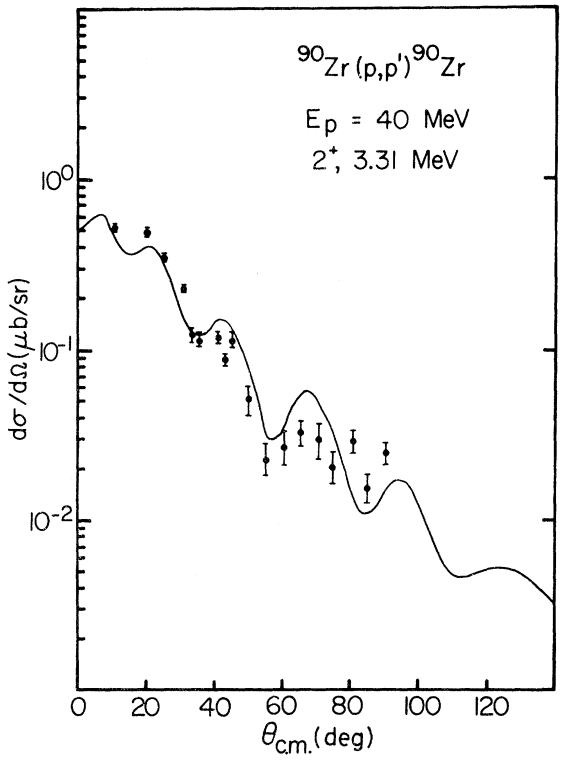

FIG. 3. Collective-model fit to the excitation of the state at 3.31 MeV, $E_p = 40.0$ MeV.

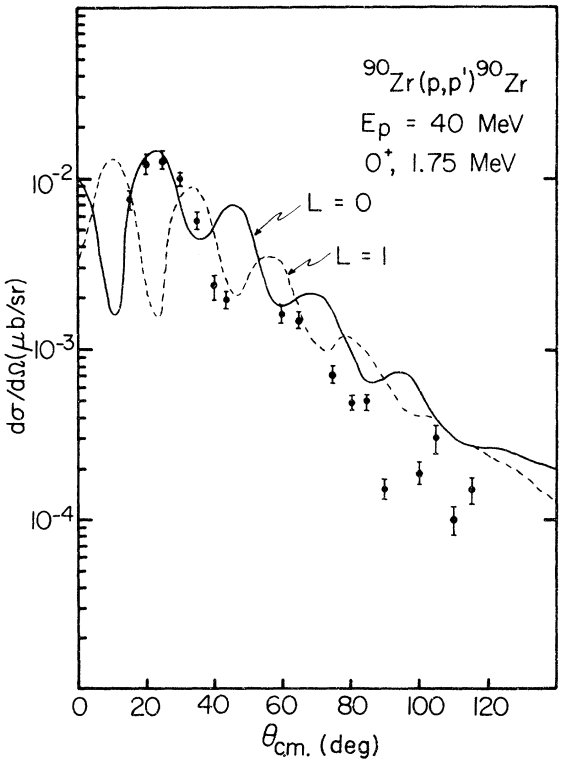

FIG. 4. $L = 0$ and $L = 1$ collective-model fits to the excitation of the 0^+ state at 1.75 MeV, $E_p = 40.0$ MeV.

of the transition density when an interaction of finite range is used. To construct these transition densities the wave functions for both the ground and excited states were taken to have the general form

$$\psi = \psi_0 + \delta\psi \,. \tag{1}$$

Here ψ_0 denotes a relatively simple shell-model state obtained, for example, from single-particle energy and single-nucleon transfer[26] considerations or from a theoretical calculation. $\delta\psi$ represents a "dressing" of ψ_0 due to core polarization[7,13-16] which is treated here in perturbation theory. For all of the even-parity states considered, ψ_0 was taken to be a pure proton configuration described by

$$|\psi_0^{J^+}\rangle = \delta_{J0}\, a_0 |(2p_{1/2})^2, J^+\rangle + b_J |(1g_{9/2})^2, J^+\rangle \,. \tag{2}$$

For the ground state a_0 and b_0 were taken to be 0.8 and 0.6, respectively; for the second 0^+ state $a_0 = -0.6$, $b_0 = +0.8$; for the other even-parity states considered, $a_J = 0$, $b_J = 1.0$. For the 5^- state at 2.32 MeV, ψ_0 was assumed to consist of two protons occupying the $2p_{1/2}$ and $1g_{9/2}$ orbitals. That part of the scattering attributed entirely to ψ_0 is termed the valence contribution; the remainder is called the core contribution.

1. *MACROSCOPIC TREATMENT OF THE CORE*

In this section, a vibrational collective model[13] is used to represent the effects of core polarization. In particular $\delta\psi$ is obtained[13] by coupling simple shell-model states of the valence nucleons to excitations of the core. The strength of the resulting core amplitudes are measured by the parameter $A_L = Y_L\langle k\rangle$ as defined in Ref. 13. The A_L were adjusted empirically until the core plus valence amplitudes together yielded the experimental cross section. No core polarization of the $S = 1$ type[13] was included.

The central part of the interaction between the valence protons and the projectile was taken to be the bare Gaussian potential of Blatt and Jackson[27] shown by Wong and Wong[28] to give matrix elements similar to those obtained from the long-range part of the Hamada-Johnston (HJ) potential.[8,29] A more complete correspondence with the HJ potential could be obtained by multiplying this Gaussian by ~0.85. This was not done. The tensor and spin-orbit components of the nucleon-nucleon force have been included for the $L = 6$ and 8 transitions. The triplet-odd part of the two-body spin-orbit (TBSO) force was taken to be that of Gogny, Pires, and de Tourreil[30] (GPT). The triplet-odd part of the tensor force was taken to be −0.30 times the strength of a triplet-even tensor[31] which fits the small momentum components of the corresponding part of the truncated HJ potential. This triplet-odd tensor force is also roughly equivalent to that used by GPT.

The knock-on exchange terms arising from the valence contributions were calculated explicitly for the central part of the interaction. When the noncentral parts of the force were included, the knock-on exchange terms associated with the tensor force were calculated explicitly; the exchange terms for the more complicated spin-orbit interaction were included approximately[12] by doubling the corresponding direct term. Core polarization

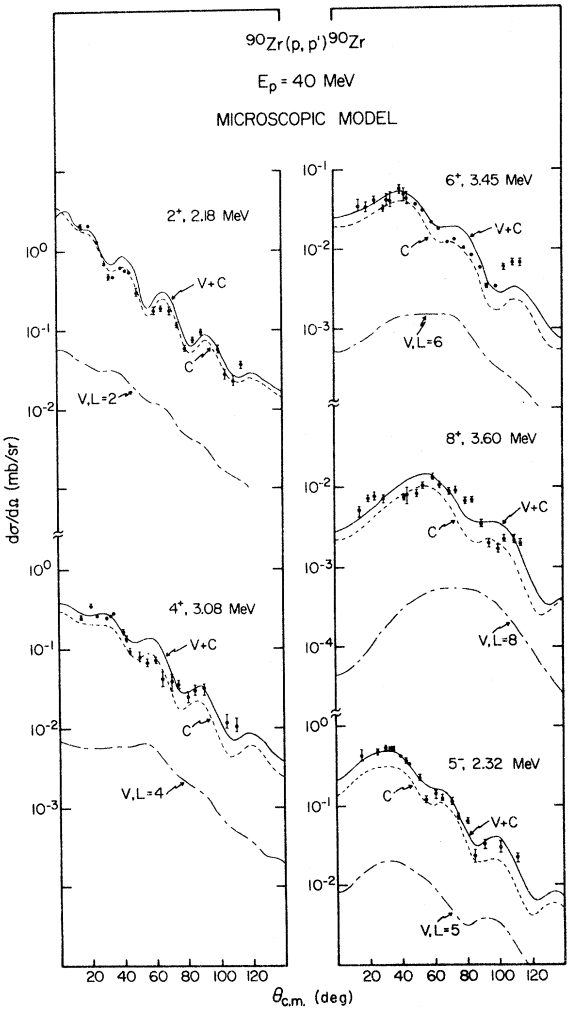

FIG. 5. Shell-model fits to the excitation of the lowest 2^+, 4^+, 6^+, 8^+, and 5^- states including macroscopic core polarization. $V(C)$ denotes the valence (core) contribution and $V + C$ denotes the coherent sum.

exchange effects of the type described by Love[32] were not included.

The shell-model orbitals were obtained by binding a proton in a Woods-Saxon well of radius $R = 1.2A^{1/3}$ fm, diffuseness $a = 0.7$ fm, and a spin-orbit coupling 25 times the Thomas term. The $1g_{9/2}(2p_{1/2})$ proton was assumed bound by 5.68(6.6) MeV. Nonlocality corrections were not included.

Lowest 2^+, 4^+, 6^+, 8^+, and 5^- States

Figure 5 shows a comparison between the experimental and calculated cross sections for these five states. The calculations in Fig. 5 include neither the noncentral components of the force nor the $S=1$ amplitudes arising from knock-on exchange. The omission of these terms has been shown[3, 12] to be relatively unimportant for the two states of lowest spin; for the 5^-, 6^+, and 8^+ states these terms were deleted to facilitate comparison with the results of Ref. 3. As found in earlier work[2, 3] the core contributions dominate the transitions and, moreover, are instrumental in obtaining angular distributions with shapes similar to the experimental data.

The core coupling strengths A_L extracted from this analysis are given in Table II along with the values determined at 61 MeV. The effective charges implied by these strengths[3, 13] when the core coupling is assumed to come from proton and neutron excitations in the ratio Z to N are also shown. The consistency of the A_L for the two different energies is not surprising, since core polarization effects dominate these transitions and the vibrational collective model alone give rise to a reasonably consistent set of β_L. As pointed out in Ref. 3, the A_2 and A_5 obtained are in reasonable agreement with the values required to explain the corresponding values of the experimental $B(E2)$ and $B(E5)$.

Since previous calculations[12] have indicated the importance of both the noncentral parts of the force (particularly the spin-orbit part) and the $S=1$ amplitudes arising from knock-on exchange for excitation of the high-spin states, calculations were made including these terms in the *valence* part of the transition amplitudes for the excitation of the 6^+ and 8^+ states. Figure 6 shows a comparison between these calculations and the experimental data, as well as a decomposition of

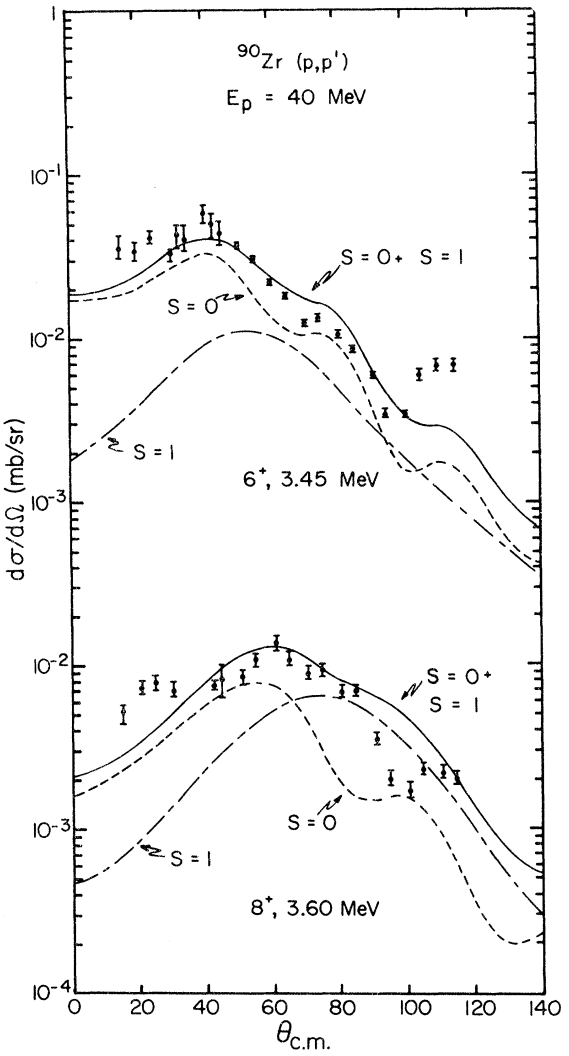

FIG. 6. Shell-model fits to the excitation of the 6^+ and 8^+ states including both core-polarization and the noncentral parts of the two-body interaction.

TABLE II. Core-coupling parameters (A_L). The number 61.2 denotes the result for 61.2-MeV protons from Refs. 3 and 12. The numbers in parentheses correspond to including both $S=1$ central force terms and the noncentral parts of the force.

State	2^+	4^+	6^+	8^+	5^-
E_{ex} (MeV)	2.18	3.08	3.45	3.60	2.32
L	2	4	6	8	5
A_L	0.166	0.092	0.056 (0.050)	0.043 (0.038)	0.051
A_L (61.2)	0.166	0.103	0.056 (0.056)	0.048 (0.036)	0.051
e_{eff}/e	2.93	2.18	1.68 (1.61)	1.42 (1.37)	1.67

the cross sections into their $S=0$ and $S=1$ parts. Although spin-orbit distortion is present in the optical potential, interference effects between the $S=0$ and $S=1$ amplitudes are small[12] so that the corresponding *cross sections* were added. The quality of the fits to the experimental data is not substantially altered by including these spin-dependent terms. There may be some slight improvement. As seen in Table II the values of both A_6 and A_8 required are reduced by roughly 10% when the spin-dependent terms are included. The corresponding reduction in A_6 for 61.2-MeV protons was undetectable, while A_8 was reduced by 25%. A large part of this discrepancy can be attributed to ambiguities in normalizing the calculated cross sections which only roughly fit the data.

It should be noted that core-polarization effects tend to quench nuclear excitations of the $S=1$ type.[7,13,16] However, S in Fig. 6 denotes spin transfer to the projectile rather than to the nucleus. For the tensor and central parts of the force these two spin-transfers must be equal[12] so that a more complete treatment of core polarization would likely reduce the $S=1$ contributions arising from these terms. For the TBSO force, however, only $S=0$ nuclear excitations give rise to amplitudes with a projectile spin transfer of unity ($S=1$). As a result, the $S=1$ type amplitudes may in fact be underestimated. In addition the $S=0$ amplitude from the spin-orbit force which is out of phase with the $S=0$ amplitude from the central force might be reduced, since it arises from $S=1$ nuclear excitations.

0^+ State at 1.75 MeV

The most striking feature of the excitation of this state is its strong dependence on the proton bombarding energy. The peak cross section of this state decreases by roughly 2 orders of magnitude in going from a proton bombarding energy of 12.7 to 40 MeV. Consequently, at a proton bombarding energy of 40 MeV, the peak cross section for this 0^+ state is only as large as that for the weakly excited 8^+ state at 3.6 MeV of excitation. By comparison, the peak cross section for exciting the first 2^+ state, for example, *increases* as the energy increases (at least up to 61.2 MeV). Such a pronounced energy dependence for the excitation of the 0^+ state strongly suggests a multiple-excitation mechanism at least at the lower bombarding energy.

With the above ideas in mind, distorted-wave calculations were performed for the 40-MeV data. The central, spin-orbit, and tensor components of the nucleon-nucleon interaction were included just as for the transitions to the 6^+ and 8^+ states. The results are shown in Fig. 7. No core-polarization effects were included, with the result that the calculated cross section is 5 times as large as the experimental one, and the shape of the cross section is rather poorly described. By comparison, the calculated cross section for a proton bombarding energy of 12.7 MeV is much *smaller* than experiment.[8] The shape of the angular distribution is poorly reproduced at that energy also.

The transition to this excited 0^+ state is particularly sensitive to the noncentral parts of the force, partly due to the fact there is a cancellation[12] between the $p_{1/2}{}^2$ and $g_{9/2}{}^2$ parts of the $S=0$ form factor for the central force, while there is constructive[12] interference between these same parts for an $S=1$ transfer to the nucleus. Including the TBSO interaction reduces the $S=0$ cross section by a factor of 3. The noncentral components of the force *enhance* the $S=1$ cross section by roughly a factor of 20. Coulomb excitation was included in the direct, $S=0$ amplitude and reduced that part of the integrated cross section by 20%.

Clearly there is a serious discrepancy between the microscopic approach used here and the experimental data. In light of the simplicity of the

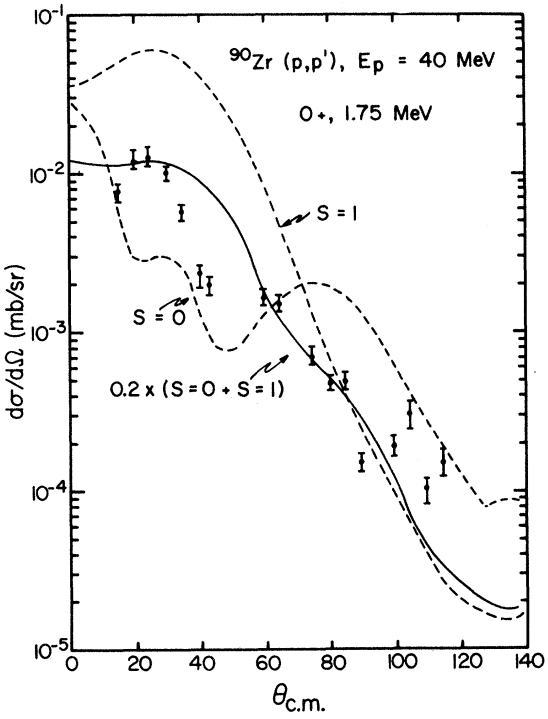

FIG. 7. Shell-model fit to the excitation of the 0^+ state at 1.75 MeV including noncentral two-body forces but no monopole core polarization as described in the text.

assumed wave functions and the strong energy dependence of the observed cross section, it appears pointless to pursue this model further without investigating the importance of multistep processes.

Multiple Excitation

Previous calculations[33] of the effects of multiple excitation suggested that this mechanism was unimportant. However, in those calculations core-polarization and exchange effects were ignored except insofar as an effective interaction of strength 200 MeV and range 1 fm was used. Using such a strong interaction is tantamount to assuming that core-polarization and exchange effects are equally important for transitions of all multipolarities. There is now evidence that while quadrupole transitions are enhanced, core-polarization effects quench[34] the monopole matrix element connecting the first and second 0^+ levels in ^{90}Zr. Consequently, it is of interest to reexamine the role of multiple excitation when realistic interactions are used and the effects of core polarization and exchange are treated explicitly.

To investigate the effects of multiple excitation, a modified version of the coupled-channels program of Tamura[20] was used. Only a simple coupling was assumed. In particular, a coupled-channels calculation was made in which the ground state, first excited 2^+ state, and first excited 0^+ (0_2^+) state were included. A more satisfactory calculation would include coupling to the strong 3^- state at 2.75 MeV of excitation. However, little is known about the magnitude of the $0_2^+ \rightarrow 3_1^-$ matrix element.

Since excitation of the first 2^+ state was found to be dominated by core polarization, a pure collective-model form factor was used for the $0_1^+ \rightarrow 2_1^+$ and $2_1^+ \rightarrow 0_2^+$ couplings.[20] The matrix element for the $0_2^+ \rightarrow 2_1^+$ transition was taken to be (0.8/0.6) times that for the $0_1^+ \rightarrow 2_1^+$ transition which is consistent with the $1g_{9/2}{}^2$ admixtures in the two 0^+ states.[26] Monopole core-polarization contributions were not included and Coulomb excitation and all spin-dependent two-body forces were neglected.

Figure 8 shows a comparison between the coupled-channels calculations and the data. The direct (D) form factor was obtained using the same central interaction and shell-model wave functions as in the distorted-wave calculations except that it was multiplied by 1.4 to roughly account for exchange. The curve labeled D was obtained by setting the coupling between the 0_2^+ and 2_1^+ states to zero, while the curve labeled M had the coupling between the 0_1^+ and 0_2^+ states set to zero. The curve labeled $M+D$ includes all couplings. Both multiple (M) and direct processes separately predict cross sections too large by a factor of 2. Together the cross section ($M+D$) is too large by a factor of 5. The shape of M, however, is in reasonable agreement with the experimental angular distribution. Both D and $M+D$ cross sections are in much poorer agreement with the data.

To see what effect multiple excitation has on the energy dependence of the cross section, similar calculations were performed at a proton bombarding energy of 12.7 MeV. At this lower energy the cross section due to multiple excitation is considerably larger than that due to direct excitation and alone accounts for about 60% of the observed cross section. This is especially true for $\theta_{c.m.} \gtrsim 110°$ where the multiple excitation cross section is roughly an order of magnitude greater than the direct. Moreover, the shape of the multiple-excitation cross section looks much more like experiment than does the direct term alone. Since the multiple cross section is too large by a factor of 2 at 40 MeV, the energy dependence of the multiple term alone is correct to within a factor of 3. Inclusion of the direct term worsens agreement with experiment which may not be surprising in view of the uncertainties associated

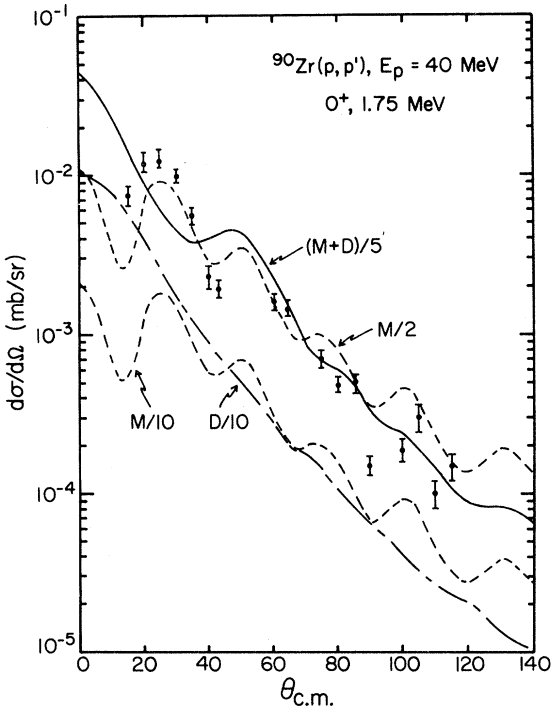

FIG. 8. A comparison of a coupled-channels calculation with the experimental cross section for the excitation of the 0^+ state at 1.75 MeV. D, M, and $M+D$ denote the direct, multiple, and multiple-plus-direct (coherent sum) cross sections, respectively.

with core-polarization effects of the monopole type, as well as the sensitivity of this transition to the weak parts of the two-body force. Nevertheless, the important role of multipole excitation seems well established.

A coupled-channels calculation was also performed in which the 4^+ level at 3.08 MeV was included in addition to the 0_1^+, 2_1^+, and 0_2^+ states. Excitation of the 0_2^+ and 2_1^+ levels were only slightly altered. Multiple excitation for the 4^+ state is relatively much less important than for the 0_2^+ state; the multiple cross section for the 4^+ level being roughly an order of magnitude smaller than experiment. However, the multiple process is of roughly the same importance as in the valence term alone. Except for the 0_2^+ level (and possibly the level at 3.31 MeV) the relatively weak energy dependence of the cross sections for the other levels suggests that multiple excitation is not important for those transitions.

2. *MICROSCOPIC TREATMENT OF THE CORE*

Completely microscopic wave functions are available for the low-lying states in ^{90}Zr.[7,35] These differ from the wave functions used in the previous section of this paper in that $\delta\psi$ is made up of many 3p-1h admixtures as compared to a single admixture obtained by coupling the valence nucleons to an "effective" macroscopic core phonon. The 3p-1h admixtures have been estimated using first-order perturbation theory. All contributing 3p-1h configurations with energies up to $2\hbar\omega$ in the case of positive-parity transitions and $1\hbar\omega$ in the case of negative-parity transitions have been included. Harmonic-oscillator radial wave functions with $\hbar\omega = 9.1$ MeV have been used in the calculations and the energy denominators have been taken from the Nilsson chart at zero deformation.

Two coupling interactions have been considered. The first is the long range part of the Kallio-Kolltveit potential (KK).[36] This is an s-state, central interaction which is a good approximation to the strong, even central components of the bound state reaction matrix derived from the HJ potential.[8,29,37] The second is a renormalized force consisting of the KK interaction plus additional P_0, P_2, P_4, P_6, and P_8 multipole-multipole components whose strengths have been fixed to match the corresponding components of the G_{3p-1h} matrix elements calculated by Kuo[38] for the low-lying configurations in ^{90}Zr. The main purpose for introducing this renormalized coupling interaction is to include some estimate of the effect of interactions between the core particles. These are quite important, at least for transitions of low multipolarity, as can be seen from the large contributions to quadrupole effective charges obtained by summing Tamm-Dancoff-approximation (TDA) and random-phase-approximation (RPA) graphs to all orders.[38] Use of the renormalized force defined above is roughly equivalent to treating the effect of core interactions in lowest order as represented by the second-order TDA graph of Siegal and Zamick.[39] Although these calculations for ^{90}Zr[7,35] are no doubt oversimplified to some degree, the resulting wave functions are expected to display the major features of the effects of core polarization.

Some idea of the properties of these wave functions can be obtained by examining the nuclear transition densities for definite orbital, spin, and total angular momentum transfer (LSJ) which are defined by

$$F_q^{LSJ}(r) = \left\langle f \left\| \sum_i \frac{\delta(r-r_i)}{r_i^2} T_{LSJ}(i) \right\| i \right\rangle . \tag{3}$$

In this equation q (=p or n) is a charge index and the sum on i runs over the protons or neutrons of the target accordingly, T_{LSJ} is the spin-angle tensor defined in Ref. 1 and $\langle \| \| \rangle$ is a reduced matrix element.[40] It is convenient to divide F_p^{LSJ} into valence and core parts and introduce the parameters

$$\lambda_p^{LSJ} = \frac{\int F_{p_c}^{LSJ}(r) r^{L+2} dr}{\int F_{p_v}^{LSJ}(r) r^{L+2} dr}, \tag{4}$$

$$\lambda_n^{LSJ} = \frac{\int F_n^{LSJ}(r) r^{L+2} dr}{\int F_{p_v}^{LSJ}(r) r^{L+2} dr} \tag{5}$$

which provide a measure of the contributions from core polarization. Observe that $1+\lambda_p^{J0J}$ is simply the effective charge. Correspondingly, the factor which gives the enhancement of an inelastic proton scattering cross section, i.e.,

$$\sigma^{LSJ} = (\epsilon_p^{LSJ})^2 \sigma_v^{LSJ},$$

is given roughly by

$$\epsilon_p^{LSJ} \approx 1 + \lambda_p^{LSJ} + \alpha_S \lambda_n^{LSJ}, \tag{6}$$

where $\alpha_S = V_{pn}^S / V_{pp}^S$ is the ratio of the p-n and p-p force strengths. This formula, which is valid only for central projectile-target interactions and normal L transfers $[\Delta\pi = (-1)^L]$, was first suggested by Atkinson and Madsen.[4] In deriving the result, shape differences amongst F_{p_c}, F_{p_v}, and F_n and between V_{pp}^S and V_{pn}^S are ignored and it is assumed that the "knock-on" exchange amplitudes are in phase with the corresponding direct ampli-

tudes – all of which are true to a good approximation.

The parameters obtained with the two sets of wave functions from Ref. 7 and 35 are summarized in Table III. Only transitions from the ground state to the first excited 2^+, 4^+, 6^+, 8^+, and 5^- states have been considered. Experimental effective charges have been included where available and experimental enhancement factors are also shown. These have been obtained by dividing the 40-MeV collective-model integrated cross sections of Sec. III B 1 by the corresponding integrated cross sections for the valence transitions calculated with the long-range part of the HJ force with exchange.[41] Contributions to the valence cross sections from exchange with non-normal L transfers $[\Delta\pi \neq (-1)^L]$ have not been included even though they are appreciable for the transitions to the higher-spin states.[8] The reason is that these $S=1$ contributions will not be enhanced as a result of core polarization (the normal transfer, $S=1$ contribution to the cross section for the 5^- state is reduced) and thus they will not be important in the final cross sections.

For the $S=0$ multipoles, in the case when interactions between the core particles are neglected, it is seen that the valence protons of ^{90}Zr polarize the core neutrons to a much greater extent than they do the core protons. This is due largely to the fact that V^0_{pn} is about 2.8 times larger than V^0_{pp}. For the same reason the scattered proton is about 2.8 times more sensitive to neutron admixtures than to proton admixtures; therefore, even though rather small polarization charges ($\delta e^J = \lambda_p^{J0J}$) are predicted, the corresponding factors for proton scattering transitions ($\delta\epsilon_p^{J0J} = \epsilon_p^{J0J} - 1$) are quite large. The values of $\delta\epsilon_p^{J0J}/\delta e^J$ range from 10 to 20. The multipole dependence of these two factors are indicated by the ratios $\delta e^2/\delta e^8$ and $\delta\epsilon_p^{202}/\delta\epsilon_p^{808}$ which are about 5 and 2.5, respectively.

The effect of core interactions is to create correlations between the core particles so that proton and neutron admixtures are not simply proportional to the strengths of the corresponding components of the valence-core interaction. It is known from TDA and RPA calculations for closed-shell nuclei[42] that the effect of the residual particle-hole interaction is to push the isoscalar component of the normal-parity particle-hole strength down in energy and to push the isovector component up in energy – these effects being most pronounced for the lower multipoles. This then explains the results of the calculations with the renormalized KK force (RKK) which give core transition densities with larger isoscalar components ($\lambda_p^{J0J} + \lambda_n^{J0J}$) and isovector components ($\lambda_p^{J0J} - \lambda_n^{J0J}$) which are reduced in magnitude relative to the results obtained with the KK force. Correspondingly δe^J and $\delta\epsilon_p^{J0J}$ both become larger, δe^J more so than $\delta\epsilon_p^{J0J}$, so that the values of $\delta\epsilon_p^{J0J}/\delta e^J$ are reduced to the range 5–10. In addition the multipole dependence of δe^J and $\delta\epsilon_p^{J0J}$ are increased. Specifically $\delta e^2/\delta e^8 \approx 10$ and $\delta\epsilon_p^{202}/\delta\epsilon_p^{808} \approx 4$.

The theoretical value of $e^2_{\rm eff}$ (RKK) falls within the experimental limits. However, the corresponding value of ϵ_p^{202} is larger than the experimental value. The theoretical values of ϵ_p^{J0J} for the other transitions fall off too fast with increasing multipolarity when compared to the experimental values. It will be seen shortly that the central imaginary and the spin-orbit components in the projectile-target interaction might explain this discrepancy. The theoretical value of $e^5_{\rm eff}$ (RKK) falls within the experimental limits. The inclusion of a P_5 component in the coupling interaction would increase this value somewhat.

TABLE III. Parameters for transition densities from microscopic wave functions.

Transition J (LSJ)	KK λ_p^{LSJ}	KK λ_n^{LSJ}	KK $e^J_{\rm eff}$	KK ϵ_p^{LSJ} [a]	Renormalized λ_p^{LSJ}	Renormalized λ_n^{LSJ}	Renormalized $e^J_{\rm eff}$	Renormalized ϵ_p^{LSJ} [a]	Experiment $e^J_{\rm eff}$ [b]	Experiment ϵ_p^{LSJ}
2^+ (202)	0.41	1.34	1.41	5.10	1.55	2.11	2.55	8.35	2.3–3.2	6.83
4^+ (404)	0.26	1.06	1.26	4.18	0.69	1.37	1.69	5.46		5.96
6^+ (606)	0.14	0.84	1.14	3.45	0.30	0.95	1.30	3.91		4.86
8^+ (808)	0.08	0.60	1.08	2.73	0.16	0.61	1.16	2.84		4.63
5^- (505) [c]	0.28	0.74	1.28	3.32	0.35	0.79	1.35	3.52	1.33–1.55	4.56
(515)	−0.25	0.05	···	0.74	−0.24	0.06	···	−0.75		···

[a] It has been assumed that $\alpha_0 = 2.75$ and $\alpha_1 = -0.20$ which are typical of the interactions being considered.

[b] See Ref. 3 for origins of data. The Woods-Saxon radial wave functions described in Sec. III C 1 and the harmonic-oscillator radial wave functions with $\hbar\omega = 9.1$ MeV give reasonably consistent values of $\langle r^2\rangle$ and $\langle r^5\rangle$. The spread of values for $e^2_{\rm eff}$ is a result of discrepancies between different experimental measurements while the spread of values for $e^5_{\rm eff}$ represents the probable uncertainty in $\langle r^5\rangle$ (Ref. 11).

[c] ϵ_p^{505} was determined from the $S=0$ valence cross section calculated with exchange treated approximately (Refs. 6, 7, and 43).

It is interesting that the values of $e^J_{\rm eff}$(RKK) are in all cases smaller than those of Table II which have been extracted from the proton scattering data using the macroscopic model for the core. This is due in part, at least for the transitions of higher multipolarity, to the fact that the macroscopic model results were interpreted under the assumption that the contributions from neutron and proton core excitations are in the ratio N to Z, while the microscopic calculations predict much weaker correlations between the core neutrons and protons. Data are available to test this point only in the case of the $J=5$ transition where the effective charge from Table II is a bit too large. In addition the two models appear to differ in regard to an important geometrical aspect. This can be seen for the $J=2$ transition where the microscopic calculation yields a slightly smaller value of $e^2_{\rm eff}$ even though it overestimates the experimental (p,p') cross section. The microscopic result is symptomatic of transition densities which peak at too small a radius and have too large a peak magnitude. In other words the proton transition density obtained in this calculation might be too large even though the effective charge predicted appears to be reasonable. The microscopic results could be brought into agreement with the macroscopic results by decreasing the magnitude of the transition densities and moving them to a larger radius. This point should be checked against experimental electron scattering data as it might have important consequences in the interpretation of all effective charge calculations.

Lowest 2^+, 4^+, 6^+, 8^+, and 5^- States

Differential cross sections have been calculated for these five transitions using the wave functions obtained with the renormalized KK force. The projectile-target interaction was taken to be the long-range part of the HJ potential[8,29,37] and "knock-on" exchange contributions were included using a zero-range approximation developed elsewhere.[6,7,43] The approximate results for normal L transfers were checked against the exact results for the valence transitions[41] and it was found that the errors introduced by this approximation were at most about 20%. Non-normal L transfers are automatically excluded by the approximation.

The results are shown as dashed curves in Fig. 9. The cross sections for the valence transitions have not been shown, since they are quite similar to those shown in Fig. 5. Also, it should be noted that the values of ϵ shown in this figure have been determined by comparison with the theoretical cross sections with and without core polarization, and not by using the approximate equation (6).

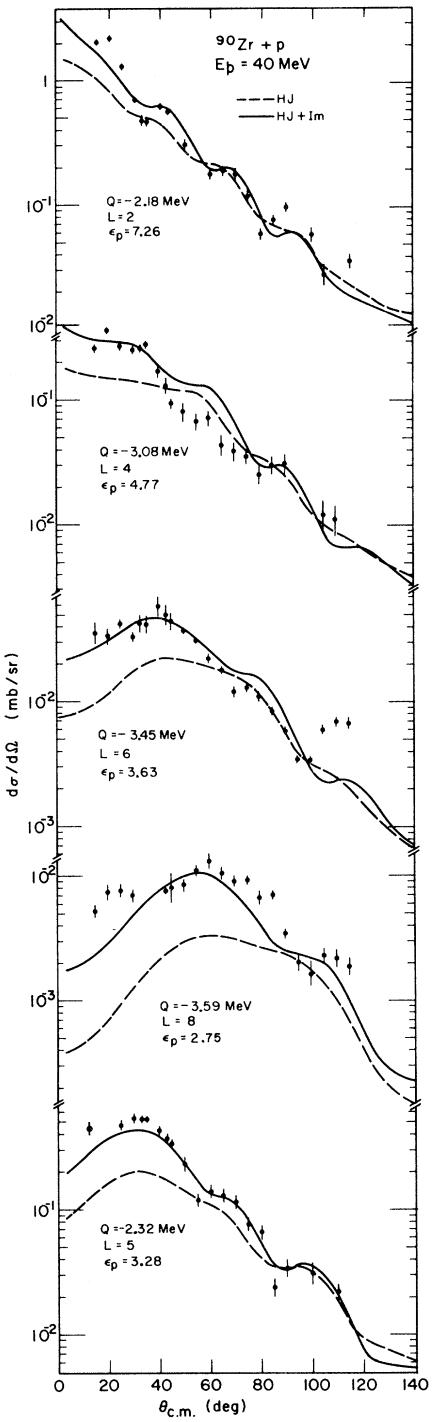

FIG. 9. Results of completely microscopic calculations for the lowest 2^+, 4^+, 6^+, 8^+, and 5^- states in ^{90}Zr for $E_p = 40$ MeV. The solid curves include a central imaginary component in the projectile-target interaction. The theoretical cross sections for the $L=2$ transition have been reduced by a factor of 2 to allow better comparison with the data.

From the figure it is seen that the magnitude of the theoretical cross sections are in agreement with the experimental cross sections within about a factor of 2.5. This has already been inferred from the discussion of the transition densities. The shapes of the theoretical cross sections are not particularly good, however.

In an effort to see if this situation could be improved, a central imaginary component was included in the projectile-target interaction as prescribed by the "frivolous" model of Satchler.[10] In these calculations the ground-state density for ^{90}Zr was assumed to have a Woods-Saxon shape with half-way radius 4.85 fm and diffuseness 0.568 fm. These parameters have been taken from elastic electron scattering data on ^{88}Sr and ^{89}Y.[44] In addition it was assumed that the p-p and p-n components of the imaginary interaction have the same shape and that their strengths are in the same ratio as the volume integrals of the long-range part of the HJ potential[8,29,37]; i.e., the p-n component is 2.58 times stronger than the p-p component. Satchler[10] did not need this assumption as he considered only $T=0$ transitions in the $N=Z$ nucleus. The motivation for the assumption made here comes from the impulse approximation where it is known that the imaginary part of the free t matrix roughly follows the strength of the real part in the 20- to 60-MeV energy region.[7] Additional information on this point might be obtained by looking at the $(N-Z)/A$ dependence of the optical potential.

The results obtained with this imaginary component included are shown as solid curves in Fig. 9. The improvement both in shape and magnitude is quite dramatic. The integrated cross sections for the 2^+, 4^+, 6^+, 8^+, and 5^- transitions have been increased by 1.29, 1.44, 1.68, 2.29, and 1.68, respectively, by including the imaginary component. The contributions from the imaginary component of the projectile-target interaction grow larger with increasing multipole because the imaginary component is assumed to have zero range,[10] while the real component has finite range. These calculations then must be considered upper limits on the effect of the imaginary component as the introduction of any finite-range dependence will reduce its effect for the higher multipolarities.

Noncentral Contributions

Completely microscopic calculations with tensor and spin-orbit components included in the projectile-target interaction have also been made. In these calculations the effect of the noncentral components of the interaction are included in both the *valence* and *core* parts of the transition amplitude. The calculations have been performed with the computer code DWBA 70[45] which allows the treatment of real interactions with central (S), tensor (T), and spin-orbit (LS) components and an exact treatment of "knock-on" exchange. This program is restricted to total angular momentum transfer $J \leq 7$, so theoretical cross sections have been calculated only for the excitation of the 2^+, 4^+, and 6^+ states. Additional restrictions in this program are that Yukawa radial forms must be used for the central and spin-orbit parts of the interaction and r^2x Yukawa radial forms must be used for the tensor part of the interaction. The precise form of the interaction used in these calculations is given in the Appendix.

The cross section for the 2^+ excitation was unaffected by including the noncentral components in the projectile-target interaction, while the

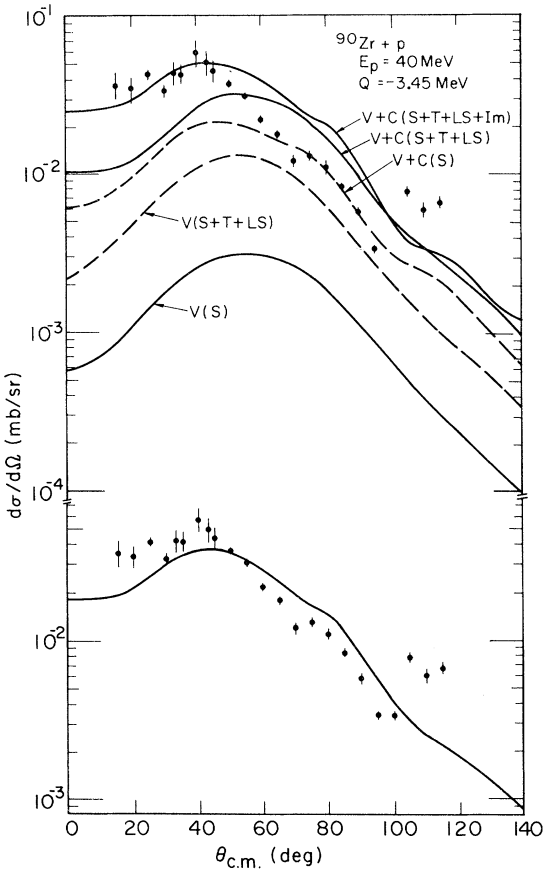

FIG. 10. Results of completely microscopic calculations for the 6^+ level in ^{90}Zr for E_p = 40 MeV with central (S), tensor (T), and spin-orbit (LS) components included in the projectile-target interaction. The upper graph shows results obtained with the RKK wave functions, and the lower graph shows results obtained with the reduced core admixtures.

cross section for the 4^+ excitation was increased only by about 20% with no significant change in shape. In the case of the 6^+ excitation the peak magnitude of the cross section was increased by about 50% and the peak was pushed out about 9°. The results for the latter are shown in the upper part of Fig. 10. Valence and valance-plus-core cross sections obtained with and without the tensor and spin-orbit parts of the interaction are shown. There are two main points to be made concerning these results. The first is that the spin-orbit force is quite important in exciting target protons and fairly weak in exciting target neutrons. This can be seen by comparing the difference between the $V(S)$ and $V(S+T+LS)$ cross sections which involve only excitation of the valence protons with the difference between the $V+C(S)$ and $V+C(S+T+LS)$ cross sections which involve neutron excitations as well as proton excitations. The second point is that the spin-orbit force gives rise to cross sections which peak at larger angles than do the cross sections arising from the central (Re + Im) parts of the force. Combining these two points it is concluded that in (p,p') transitions where the spin-orbit force is important, proton and neutron excitations are characterized by different shape contributions to the core section.

Although it was not possible to include the central imaginary part of the interaction in these calculations, its effect has been estimated by adding the difference between the Re and Re + Im results for the 6^+ excitation from Fig. 9 to the $V+C(S+T+LS)$ result in Fig. 10 which gives the curve labeled $V+C(S+T+LS+\mathrm{Im})$. This would be strictly correct if there was no interference between $S=0$ amplitudes from the central and spin-orbit parts of the force. Since there is in fact some destructive interference[12] the result is only an upper limit.

The agreement between theory and experiment for the 6^+ excitation has been worsened by including the noncentral components in the projectile-target interaction. The resulting theoretical cross section is too large between 40 and 100°. One can conclude that the strength of the spin-orbit force has been overestimated in these calculations. This can only be tested by additional calculations for other transitions. If one accepts the strength of the spin-orbit force then the discrepancy can be removed by decreasing the core contributions to the cross section. The lower part of Fig. 10 shows the result obtained by excluding core admixtures from the wave functions so as to decrease λ_p^{606} and λ_n^{606} by 80 and 20%, respectively. The result shows acceptable agreement with experiment. It is interesting that Bertsch[46] has indicated that a spin-orbit component in the valence-core coupling interaction will tend to reduce the estimates of core admixtures made with central forces alone as is the case for the wave functions used here.[7,35] Finally, it is noted that the spin-orbit force assumed here favors $\lambda_n^{606}/\lambda_p^{606} > N/Z$ as predicted by the microscopic wave functions. An increase in λ_p^{606} relative to λ_n^{606} would introduce too much backward-angle cross section. This is further evidence that the values of e_{eff} given in Table II may be too large for the higher multipoles.

Wave functions are also available for the transition to the first excited 0^+ state in ^{90}Zr.[7,35] In a previous calculation[7] it was found that the core admixtures in these wave functions enhanced the valence transition. In view of the recent evidence concerning the quenching of the monopole matrix element for this transition[34] and the importance of multiple excitation, it did not seem reasonable to pursue further calculations with these wave functions.

IV. CONCLUSION

The deformation parameters for the first 2^+, 4^+, 6^+, 8^+, and 5^- excitations in ^{90}Zr obtained in the present experiment at 40 MeV are quite consistent with those obtained in previous experiments at 18.8 and 61.2 MeV[1,3] with the possible exception of the value for β_8 extracted from the 18.8-MeV data. Deformation parameters from the 12.7-MeV data are consistently higher than those obtained at the other energies. The value of β_0 obtained at 12.7 MeV for the excitation of the first excited 0^+ state in ^{90}Zr is 10 times larger than the value obtained in the present experiment. Multiple excitation of this state through the first 2^+ state is found to be important, but the calculation made here does not explain the experimental data completely.

Microscopic model calculations have been made for the first 2^+, 4^+, 6^+, 8^+, and 5^- states using a phenomenological macroscopic treatment of core polarization, as well as a perturbative microscopic treatment of core polarization. The core coupling constants deduced from the data using the macroscopic treatment of the core were found to be consistent with those obtained from a previous analysis of the 61.2-MeV data.[3] The results of the theoretical calculations using the microscopic treatment of the core were found to be in quite good agreement with the experimental data. The main points about these calculations are that they involve no free parameters and that the interaction between the valence nucleons and the core is consistent with the real part of the projectile-target interaction.

The inclusion of an imaginary central component

in the projectile-target interaction was found to be important in improving the shape of the theoretical cross sections obtained in the completely microscopic calculations. The addition of a spin-orbit component in the projectile-target interaction led to an increase in the magnitude of the theoretical cross sections in the case of the 6^+ and 8^+ excitations, i.e., smaller core-polarization contributions are required to reproduce the data if this component of the interaction is included. In addition it was noted that the presence of the spin-orbit interaction might provide some indication, or limits, on the ratio of proton to neutron excitations which contribute to transitions which require large angular momentum transfer.

ACKNOWLEDGMENTS

The authors would like to thank G. R. Satchler, T. T . S. Kuo, and S. M. Austin for the use of unpublished results, and R. Schaeffer and J. Raynal for the use of the computer code DWBA 70.

APPENDIX

In the microscopic calculations made with the code DWBA 70 the projectile-target interaction was taken to be of the form

$$t_{pq} = V^0_{pq}(r_{pq}) + V^1_{pq}(r_{pq})\vec{\sigma}_p \cdot \vec{\sigma}_q + V^T_{pq}(r_{pq})S_{pq} + V^{LS}_{pq}(r_{pq})\vec{L}_{pq} \cdot \vec{\sigma}_{pq}, \tag{A1}$$

where $q = p$ or n,

$$V^S_{pq}(r_{pq}) = V^S_{pq}Y(r_{pq}, u_s),$$
$$V^T_{pq}(r_{pq}) = V^T_{pq}r_{pq}^2 Y(r_{pq}, u_t), \tag{A2}$$
$$V^{LS}_{pq}(r_{pq}) = V^{LS1}_{pq}Y(r_{pq}, u_{LS1}) + V^{LS2}_{pq}Y(r_{pq}, u_{LS2}),$$

with

$$Y(r, u) = \frac{e^{-r/u}}{r/u}, \tag{A3}$$

and

$$S_{pq} = 3(\vec{\sigma}_p \cdot \hat{r}_{pq})(\vec{\sigma}_q \cdot \hat{r}_{pq}) - \vec{\sigma}_p \cdot \vec{\sigma}_q,$$
$$\vec{L}_{pq} = (\vec{r}_p - \vec{r}_q) \times (\vec{p}_p - \vec{p}_q), \tag{A4}$$
$$\vec{\sigma}_{pq} = \vec{\sigma}_p + \vec{\sigma}_q.$$

The range parameters are $u_s = 1.06$ fm, $u_T = 0.816$ fm, $u_{LS1} = 0.557$ fm, and $u_{LS2} = 0.301$ fm. The strength parameters are $V^0_{pp} = -14.5$ MeV, $V^1_{pp} = 14.6$ MeV, $V^0_{pn} = -36.4$ MeV, $V^1_{pn} = -2.39$ MeV, $V^T_{pp} = -V^T_{pn} = 11.0$ MeV fm^{-2}, $V^{LS1}_{pp} = 29.1$ MeV, $V^{LS2}_{pp} = -1490$ MeV, $V^{LS1}_{pn} = 20.1$ MeV, and $V^{LS2}_{pn} = -752$ MeV.

The parameters for the central part of the interaction have been chosen to match the low-momentum components of the long-range part of the HJ potential,[8,29,37] the parameters for the tensor part of the interaction have been chosen to match the low-momentum components of the one-pion-exchange-potential tensor force,[47] and the parameters for the spin-orbit part have been chosen to match the low-momentum components of the corresponding part of the HJ potential[29] set to zero inside the hard core.[47] The J_4 integral for the isoscalar component of the latter is 8.7 MeV fm^5 which is quite close to the value of 9.6 MeV fm^5 for the force used in the calculations of Sec. III C 1. This is also roughly the value required to reproduce in first order the correct strength for the spin-orbit part of the optical potential if the direct and exchange contributions are comparable.

---

†Present address: Department of Physics, State University of New York, Oswego, New York 13126.

‡Present address: Neutron Physics Division, Oak Ridge National Laboratory, Oak Ridge, Tennessee 37830.

§Research sponsored in part by the National Science Foundation.

¶Research sponsored in part by the Research Corporation.

‖Research sponsored in part by the National Science Foundation. (Grant No. GP-22559).

**Research sponsored in part by the U. S. Atomic Energy Commission.

[1]W. S. Gray *et al.*, Phys. Rev. 142, 735 (1966); M. B. Johnson, L. W. Owen, and G. R. Satchler, *ibid.* 142, 748 (1966).

[2]J. K. Dickens, E. Eichler, and G. R. Satchler, Phys. Rev. 168, 1355 (1968).

[3]M. L. Whiten, A. Scott, and G. R. Satchler, Nucl. Phys. A181, 417 (1972).

[4]K. A. Amos, V. A. Madsen, and I. E. McCarthy, Nucl. Phys. A94, 103 (1967); J. Atkinson and V. A. Madsen, Phys. Rev. Letters 21, 295 (1968); Phys. Rev. C 1, 1377 (1970).

[5]D. A. Agassi and R. Schaeffer, Phys. Letters 26B, 703 (1968); R. Schaeffer, Nucl. Phys. A132, 186 (1969); Ph.D. thesis, Orsay, unpublished (1969); D. Larson, S. M. Austin, and B. H. Wildenthal, Phys. Rev. to be published.

[6]F. Petrovich, H. McManus, V. A. Madsen, and J. Atkinson, Phys. Rev. Letters 22, 895 (1969).

[7]F. Petrovich, Ph.D. thesis, Michigan State University, unpublished (1971).

[8]W. G. Love, L. W. Owen, R. M. Drisko, G. R. Satchler, R. Stafford, R. J. Philpott, and W. T. Pinkston, Phys. Letters 29B, 478 (1969); W. G. Love and G. R. Satchler, Nucl. Phys. A159, 1 (1970).

[9]G. R. Satchler, Comments Nucl. Particle Phys. 5, 39 (1972).

[10]G. R. Satchler, Phys. Letters 35B, 279 (1971).

[11]R. H. Howell and G. R. Hammerstein, Nucl. Phys. A192, 651 (1972).
[12]W. G. Love, Phys. Letters 35B, 371 (1971); Nucl. Phys. A192, 49 (1972).
[13]W. G. Love and G. R. Satchler, Nucl. Phys. A101, 424 (1967); G. R. Satchler and W. G. Love, *ibid.* A172, 449 (1971).
[14]B. M. Preedom, C. R. Gruhn, T. Y. T. Kuo, and C. J. Maggiore, Phys. Rev. C 2, 166 (1970).
[15]W. Benenson, S. M. Austin, P. J. Locard, F. Petrovich, J. Borysowicz, and H. McManus, Phys. Rev. Letters 24, 907 (1970); A. Scott, M. Owais, and F. Petrovich, to be published.
[16]D. Agassi and R. Schaeffer, Nucl. Phys. A145, 401 (1970).
[17]C. M. Lederer, J. M. Hollander, and I. Perlman, *Table of Isotopes* (Wiley, New York, 1967), 6th ed.
[18]M. P. Fricke *et al.*, Phys. Rev. 156, 1207 (1967).
[19]G. R. Satchler, Nucl. Phys. 77, 481 (1966).
[20]T. Tamura, Rev. Mod. Phys. 37, 679 (1965).
[21]C. R. Bingham, M. L. Halbert, and R. H. Bassel, Phys. Rev. 148, 1174 (1968).
[22]W. G. Love and L. W. Owen, Phys. Letters 37B, 463 (1971).
[23]W. G. Love, Particles Nuclei 3, 318 (1972).
[24]M. Toyama, Phys. Letters 38B, 147 (1972); R. Schaeffer and G. R. Bertsch, *ibid.* 38B, 159 (1972).
[25]E. R. Flynn, A. G. Blair, and D. D. Armstrong, Phys. Rev. 170, 1142 (1968).
[26]B. M. Preedom, E. Newman, and J. C. Hiebert, Phys. Rev. 166, 1156 (1968).
[27]J. M. Blatt and J. D. Jackson, Phys. Rev. 76, 18 (1949).
[28]C. W. Wong and C. Y Wong, Nucl. Phys. A91, 433 (1967).
[29]T. Hamada and I. D. Johnston, Nucl. Phys. 34, 382 (1962).
[30]D. Gogny, P. Pires, and R. de Tourreil, Phys. Letters 32B, 591 (1970).
[31]W. G. Love, L. J. Parish, and A. Richter, Phys. Letters 31B, 167 (1970).
[32]W. G. Love, Nucl. Phys. A127, 129 (1969).
[33]W. G. Love, G. R. Satchler, and T. Tamura, Phys. Letters 22, 325 (1966).
[34]D. Burch, P. Russo, H. Swanson, and C. G. Adelburger, Phys. Letters 40B, 357 (1972).
[35]F. Petrovich, H. McManus, and J. Borysowicz, to be published.
[36]A. Kallio and K. Kolltveit, Nucl. Phys. 53, 87 (1964).
[37]G. E. Brown, *Unified Theory of Nuclear Models and Nucleon-Nucleon Forces* (North-Holland, Amsterdam, 1967), 2nd ed.
[38]T. T. S. Kuo, unpublished.
[39]S. Siegal and L. Zamick, Nucl. Phys. A145, 1 (1970).
[40]D. M. Brink and G. R. Satchler, *Angular Momentum* (Oxford U. P., Oxford, England, 1962).
[41]G. R. Satchler, private communication.
[42]See, for example, V. Gillet and N. Vinh Mau, Nucl. Phys. 54, 321 (1964).
[43]W. G. Love, to be published.
[44]G. A. Peterson and J. Alster, Phys. Rev. 166, 1136 (1966).
[45]R. Schaeffer and J. Raynal, unpublished.
[46]G. F. Bertsch, in *The Two-Body Force in Nuclei*, edited by S. M. Austin and G. M. Crawley (Plenum, New York, 1972), p. 243.
[47]R. Schaeffer and S. M. Austin, unpublished.

PHYSICAL REVIEW C VOLUME 7, NUMBER 5 MAY 1973

Rules for Spin and Parity Assignments Based on Log*ft* Values*

S. Raman and N. B. Gove
Oak Ridge National Laboratory, Oak Ridge, Tennessee 37830
(Received 25 October 1972)

A survey was made of log*ft* values for forbidden β transitions. Three cases, ^{90m}Y, ^{65}Ni, and ^{144}Pm decays, were examined experimentally. A number of low log*ft* values reported in the literature are superseded by more recent larger values. Empirical rules for making spin and parity assignments from log*ft* values are proposed.

I. INTRODUCTION

Since the comparative β-decay half-life or *ft* value was first introduced,[1] spin and parity assignments for nuclear energy levels have been made on the basis of log*ft* values. Of the ≈6500 definite or tentative J^π assignments that now exist in the *Nuclear Data Sheets*,[2] ≈1000 depend at least partly on log*ft* values. The existing rules[3] have evolved from previous compilations of log*ft* values.[4-6] The justification for such rules tends to be slightly circular since the β classifications (allowed, first-forbidden, etc.) employed in support of a rule may, in fact, have been assigned employing that rule or a similar rule. In 1963, Gleit, Tang, and Coryell[4] found only 46 cases where the forbiddenness category[7] could be obtained without any resort to log*ft* values. The situation has since improved.

In the present study, we have evaluated and compiled into five tables and one histogram β transi-